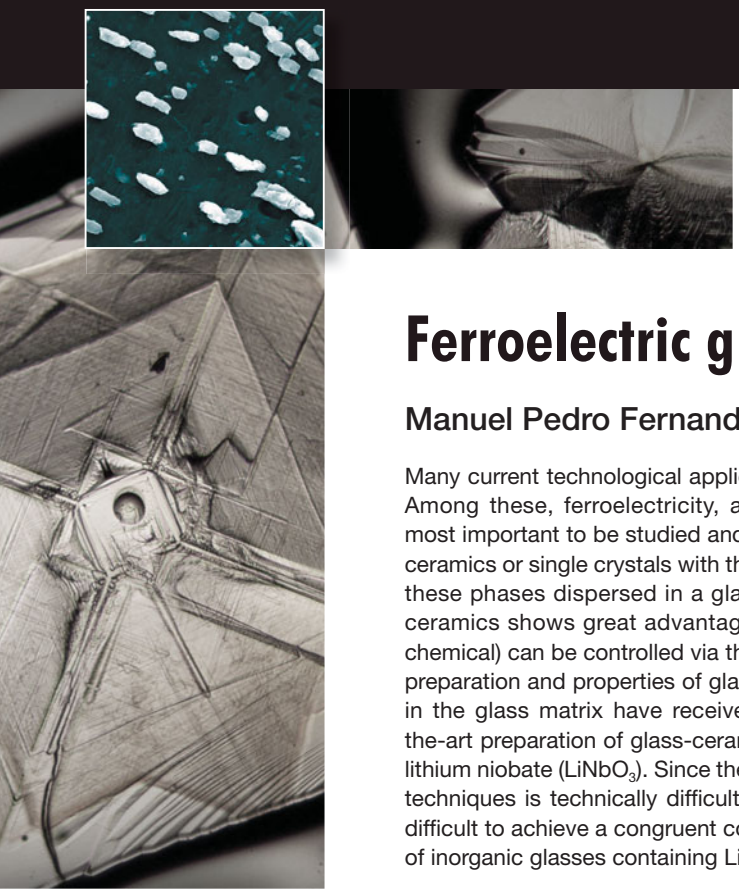


Ferroelectric glass-ceramics

Manuel Pedro Fernandes Graça and Manuel Almeida Valente

Many current technological applications are based on the electrical properties of materials. Among these, ferroelectricity, antiferroelectricity, paraelectricity, and resistivity are the most important to be studied and controlled. To overcome important drawbacks of sintered ceramics or single crystals with these characteristics, the preparation of glass-ceramics with these phases dispersed in a glass matrix is a possible solution. The formation of glass-ceramics shows great advantages—their properties (optical, electrical, mechanical, and chemical) can be controlled via the volume fraction of the dispersed active phase. Thus, the preparation and properties of glass-ceramics containing ferroelectric crystallites embedded in the glass matrix have received considerable interest. This article discusses state-of-the-art preparation of glass-ceramics with one important technological ferroelectric crystal, lithium niobate ($LiNbO_3$). Since the preparation of $LiNbO_3$ single crystals by traditional growth techniques is technically difficult and economically costly—and with dense ceramics, it is difficult to achieve a congruent composition—scientific research on the fabrication methods of inorganic glasses containing $LiNbO_3$ crystallites is an important current topic.

Ferroelectric glass-ceramics—An overview

The formation of glass-ceramics has advantages when compared to ceramics and single crystals, through the possibility of controlling physical properties, namely, electrical and optical properties, by controlling the volume fraction of the active phase dispersed in the glass matrix (please see the Introductory article in this issue). For example, to maintain optical transparency, the process of nucleation and crystal growth requires great control when the size of crystals dispersed in the glass matrix are not large enough to cause light scattering. However, for most electrical applications, it is necessary that the crystals have a size sufficient to present, for example, a ferroelectric response. These two attributes represent a difficult tradeoff. One solution to ensure optical transparency exploits the small difference between the refractive indices of crystals and glass matrix. If this difference is negligible, it allows, regardless of the crystal size, maintenance of the optical transparency of the glass-ceramic.

Ferroelectricity—General principles

Interest in ferroelectric materials results from its broad spectrum of technological applications. Ferroelectricity was discovered in the 17th century by E. Seignette, in La Rochelle, France, during the study of $NaKC_4H_4O_6.4H_2O$, known as Rochelle salt. In 1824, D. Brewster found that this material responded electrically to thermal stimuli, a phenomenon known as pyroelectricity. Later, in 1880, Pierre and Paul Curie characterized the response of this salt, and other crystals such as quartz, sphalerite (ZnS), and tourmaline ((Ca, K, Na, [])(Al, Fe, Li, Mg, Mn)$_3$(Al, Cr, Fe, V)$_6$(BO$_3$)$_3$(Si, Al, B)$_6$O$_{18}$(OH, F)$_4$), to the effect of pressure (mechanical stimulation) to generate electrical polarization, resulting in the discovery of piezoelectricity.[1]

In 1918, W. Anderson and J. Cady[2,3] observed an anomaly in the piezoelectric characteristics of Rochelle salt, indicating that the linearity between polarization and external field becomes invalid for high electric fields. In 1921, J. Valasek noticed that the spontaneous polarization presented by Rochelle salt could be reversed by the action of an external electric field.[4] It was described, for the first time, as the phenomenon of ferroelectricity, a term adopted from ferromagnetism in reference to the hysteresis behavior they share. With the discovery of ferroelectricity in barium titanate ($BaTiO_3$) single crystals in 1940, scientific research grew exponentially in this field due to promising applications in the electronics industry, particularly in the production of computer components. This discovery led to a better understanding of the phenomenon because of the simplicity of the barium titanate structure, a perovskite. In the 1950s, a new class of ferroelectric materials was discovered: $Ba(Ti, Sn)O_3$ compounds, called relaxors. This anomalous behavior was measured.[5]

Manuel Pedro Fernandes Graça, Institute of Nanostructures, Nanofabrication, and Nanomodeling, Universidade de Aveiro, Portugal; mpfg@ua.pt
Manuel Almeida Valente, Institute of Nanostructures, Nanofabrication, and Nanomodeling, Universidade de Aveiro, Portugal; mav@ua.pt
doi:10.1557/mrs.2017.32

© 2017 Materials Research Society

https://doi.org/10.1557/mrs.2017.32 Published online by Cambridge University Press

From a physical point of view, ferroelectricity is a characteristic of certain polar materials that, in a given temperature range, presents a spontaneous polarization (i.e., the dipolar momenta per volume unit tend to align themselves in the absence of an external electric field and their polarization can be reversed by the application of an external electric field). In traditional dielectric materials, the polarization is a linear function of the applied electric field. In ferroelectric materials, the nonlinear dependence between polarization and applied field results in a hysteresis curve, as shown in **Figure 1**.[6] Three major parameters are shown: (1) P_{sat} is the saturation polarization or spontaneous polarization, which is the maximum polarization achieved by the material; (2) E_c is the coercive electric field in which polarization is zero ($P = 0$) when it is applied; and (3) P_r is the remanent polarization, when the external applied electric field is zero ($E = 0$).

Another intrinsic characteristic of ferroelectric materials is the transition temperature, known as the Curie temperature (T_C). Above T_C, the ferroelectric behavior ceases, and the material becomes paraelectric (i.e., no spontaneous polarization).

It has been assumed that the ferroelectric behavior of a material originates in the small distortion of the paraelectric phase crystal structure. The degree of symmetry of the ferroelectric phase is always less than that of the paraelectric phase. For example, in perovskites, the material has a cubic structure at temperatures higher than T_C. With decreasing temperature, the atoms of the unit cell move from the center-symmetric position, giving rise to electrical dipoles[6] and thus spontaneous polarization. Below T_C and in the absence of an applied electric field, the electric dipoles are not oriented in the same direction throughout the material, but are oriented only within a region called the ferroelectric domain.[7] These domains are randomly arranged, canceling each other and producing a null total macroscopic polarization. Application of an external electric field tends to orient the domains in the same direction, polarizing the entire material up to a maximum value (saturation polarization). Upon removal of the external electric field, most of the domains tend to remain oriented, producing a memory effect (remanent polarization).

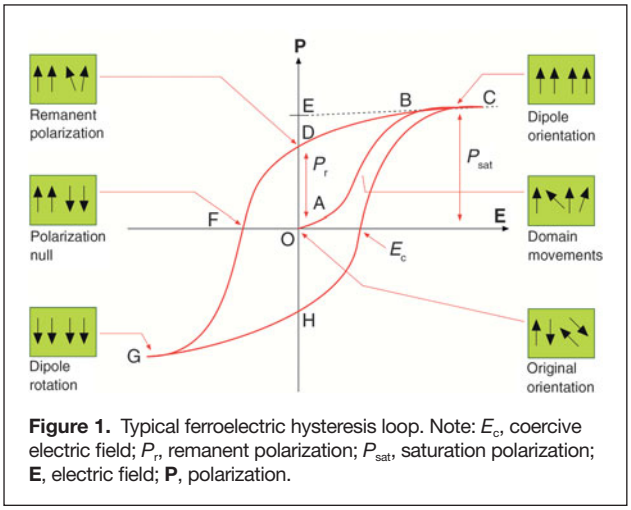


Figure 1. Typical ferroelectric hysteresis loop. Note: E_c, coercive electric field; P_r, remanent polarization; P_{sat}, saturation polarization; **E**, electric field; **P**, polarization.

As previously mentioned, among the ferroelectric materials, the ferroelectric–paraelectric transition for relaxors does not occur at a characteristic temperature, but rather, over a temperature range. Because the frequency dependence of the maximum temperature of the dielectric constant (T_m) cannot be described by the Curie-Weiss Law,[8] the scientific community proposed the following model to explain the "relaxor" behavior. Nanopolar regions of lower structural symmetry are immersed in a nonpolar matrix with structure symmetry.[8] These regions are detected at temperatures above T_m, but as the temperature decreases, an increase in these nanopolar regions may result without achieving sufficient dimensions to form ferroelectric domains.[8–12]

$LiNbO_3$ ferroelectric crystals embedded on a glass matrix

The $LiNbO_3$ crystal—Background

The most widely studied ferroelectric materials have the perovskite structure—their technological applications are based not only on their ferroelectric properties, but also on their ferromagnetic properties and superconductivity, all of which can present simultaneously. Among perovskite ferroelectric materials, lithium niobate ($LiNbO_3$), first synthesized in 1949 by Matthias and Remeika,[13] has many important applications. In the late 1960s, due to the development of various applications of $LiNbO_3$ in optical fibers, Bell Laboratories[14] initiated a detailed study on the structure and properties of the $LiNbO_3$ crystal, particularly its electro-optical properties.[15] This crystal is characterized by a high Curie temperature ($T_C = 1210$°C), a high dielectric constant (80 at 100 kHz), low dielectric losses (~0), and high resistivity (>10^{21} Ω cm) at room temperature.[13–15] It also shows high efficiency in nonlinear optics, especially in the generation of second harmonic light,[16] and is widely used as a waveguide modulator and optical switcher.[13,17,18]

The properties of this crystal have been improved with the incorporation of dopants[19–30] and the use of different preparation methods. However, due to difficulties and costs in the preparation of ferroelectric crystals, the preparation of glasses and glass-ceramics containing these crystals did not begin until the 1970s.[31–33] The advantages of glasses containing ferroelectric crystals as compared to crystals prepared by traditional methods (e.g., the Czochralski technique[34,35] or sintering) stems from the simplicity of preparation and the possibility of modifying the properties of these glasses by changing the morphology of the precipitated crystals, namely their size, shape, and volume fraction.[36] However, it is important to recognize that in general, the properties of glass-ceramics with embedded crystals are not as good as their single crystal counterparts, because the glass-ceramics present at least two phases, the crystalline (considered the active phase) and the amorphous phase.

For example, electric polarization of crystals embedded in a glassy matrix is difficult and requires higher external fields,

https://doi.org/10.1557/mrs.2017.32 Published online by Cambridge University Press

due to the low dielectric constant of the amorphous phase. On the other hand, because of the high costs associated with single-crystal growth processes, their substitution by lower cost glass-ceramics is a current topic. When compared to ceramic materials, glass-ceramics have the advantage of being high-density materials without porosity.

The best-known glass preparation method is melt quenching, which involves mixing of the raw materials and mixtures, placing them into a nonreactive crucible under melting conditions. Subsequently, by rapidly cooling the melt, a glass forms.[37] This relatively simple process yields glasses with a low degree of porosity and allows the opportunity to fabricate glass-ceramics.

For glass-ceramics, the growth and crystal orientation can generally be achieved through different processes, such as mechanical deformation, thermodynamic control, and kinetic control (electrochemically induced nucleation, which promotes the formation of nuclei in the vicinity of an electrode (cathode), due to a specific current flow, consequently inducing subsequent crystalline growth in the direction of this electrical current).[38] Thermodynamic control is the most common technique used for glasses. However, control of crystallization with the desired crystalline phase is often difficult because crystallization is a complex process affected by factors such as composition, surface conditions, and heat-treatment parameters.

Glass matrices

Different glass matrices have been used for crystallizing ferroelectric crystals, such as TeO_2,[39] SiO_2,[40–42] B_2O_3,[43] and P_2O_5.[44,45] Komatsu et al.[39] were pioneers in the synthesis of the TeO_2-Li_2O-Nb_2O_5 glass system. Using heat treatment, $LiNbO_3$ crystals were precipitated within the glass network. TeO_2 as a glass-network former is a good choice due to its low melting temperature, between 900 and 1200°C and its refractive index (~2.0), which is close to the refractive index of $LiNbO_3$ crystal (~2.2[13]), facilitating the formation of transparent glass-ceramics.[46] These researchers found that glasses with a high concentration of Li^+ (>30 mol% Li_2O), when thermally treated, resulted in a transparent glass-ceramic with $LiNbO_3$ crystals with dimensions of nearly 10 µm.[47] The main properties observed in these glass-ceramics were high values of the dielectric constant (~150), efficient generation of the second harmonic, and high nonlinear third-order coefficients.[47,48]

Shankar et al. showed that a composition containing 50% molar TeO_2 and equal amounts each of Li_2O and Nb_2O_5, heat-treated at 200°C for 12 h, formed $LiNbO_3$ crystals, which precipitated mainly on the glass surface.[49] Ding et al. studied the crystallization of $55TeO_2$-$25Li_2O$-$20Nb_2O_5$ (mol%) glass that underwent an ultrasonic treatment (28 kHz, 150 W), which promoted the nucleation and growth of $LiNbO_3$ crystals on the glass surface.[50] Kim et al. attempted the preparation of transparent glass-ceramics for the glass composition $80TeO_2$-$(20-x)Li_2O$-xNb_2O_5 (mol%), where $LiNbO_3$ crystals were incorporated. By adding 15 wt% $LiNbO_3$ to the glass and then melting it at 950°C, they obtained a transparent glass-ceramic containing lithium niobate crystalline phase.

Prasad and colleagues published a study on the preparation of glass-ceramics from the SiO_2-Li_2O-Nb_2O_5 system. SiO_2 was chosen as a network former because it does not contain cations that can change the crystal structure of $LiNbO_3$, a desirable trait for a glass former. SiO_2 satisfies this condition due to the reduced value of atomic radius and coordination number.[40–47] Todorovic et al.[47] subsequently showed the glass-forming region of the pseudo-ternary system (SiO_2-Al_2O_3)-Li_2O-Nb_2O_5, using the melt-quenching method (**Figure 2**). When $[Nb_2O_5]/[SiO_2] > 1$ and the molar amount of $[Li_2O] > 25\%$, the glasses obtained are transparent and homogeneous. Subsequent thermal treatments to these glasses promoted the crystallization of $LiNbO_3$ particles with sizes ranging between 150 and 350 nm while maintaining transparency. These glass-ceramics have a refractive index of 1.84–1.93 and a dielectric constant of 155–185 (@ 1 kHz; 300 K). Increasing the temperature and thermal treatment time led to an increase in particle size and consequent opacity of the samples.[47] Prasad et al.,[40] Hasdemir et al.,[51] and Todorovic et al.[47] studied silicate networks containing crystals of $LiNbO_3$ and concluded that homogeneous and transparent glasses occur in the region of 32–39 mol% of SiO_2.

Nonsilicate glass families have also been explored, including those based on phosphorus. Pure phosphate glasses are extremely hygroscopic and colorless, and present a refractive index close to 1.55.[52] Araujo et al.[45] prepared a series of glasses by melting compositions in the $((xNb_2O_5$-$(0.5-x)P_2O_5)$-$0.5Li_2O)$-$yFe_2O_3)$ family to study the influence of the niobium oxide to lithium oxide ratio in a phosphate glass; iron oxide was used as an impurity. Based on x-ray diffraction (XRD) and infrared spectroscopy analyses, samples with $x < 0.2$ showed no crystalline phases, and for $x > 0.2$, $LiNbO_3$ crystals

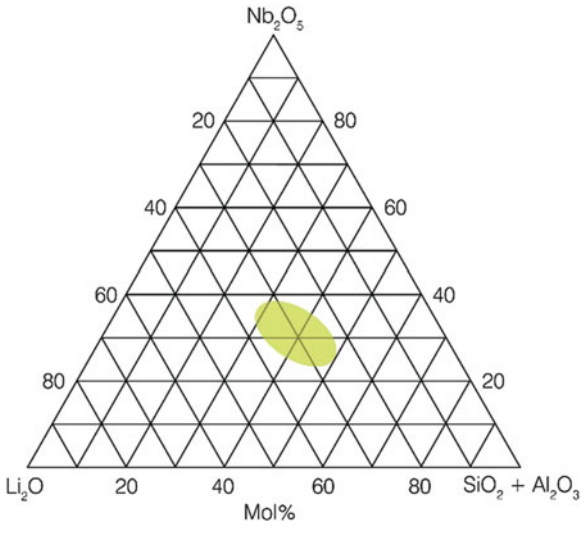


Figure 2. Glass-forming region (in green) of the Li_2O-Nb_2O_5-SiO_2-Al_2O_3 system.[47]

https://doi.org/10.1557/mrs.2017.32 Published online by Cambridge University Press

were precipitated. Chowdari et al. fabricated a series of glasses from the P_2O_5-Li_2O-Nb_2O_5 system by melt quenching, identifying the glass-formation region.[53] Araujo et al. described the doping of niobiophosphate glasses with iron.[45] The nucleation and crystal growth of ferroelectric $LiNbO_3$ in this glass matrix occurred preferentially in samples with high concentrations of niobium. In samples with lower amounts of niobium, formation of lithium phosphate phases were observed.

Singh et al.[54] showed that the preparation of lithium borate glasses ($42.5Li_2O$-$57.5B_2O_3$ in mol%) with niobium (more than 15% of Nb_2O_5) yielded crystalline phases. The Nb^{5+} ions occupy Li sites and thus the number of empty sites will increase to maintain charge neutrality. According to Tuller,[55] this type of structural rearrangement, where there are more empty sites than ions available to fill them, favors the increase of ionic conductivity. In glasses with more than 5% $LiNbO_3$, the conductivity increases, attributed to the high mobility of Li^+ ions, which is related to the increased number of empty sites. However, if the random network model proposed in 1932 by Warren and Zachariasen for silicate glasses[37,56] is suitable for lithium borate glasses, it is expected that the lithium ions will occupy empty spaces in a random manner and result in a distribution of activation energies for the conduction process. This concept was one of several that do not entirely explain the experimental observations. To explain the experimental observations, Porai-Koshits proposed in 1959 the existence of a polymer–crystalline structure, suggesting that the glassy network does not present absolute disorder.[37,56]

Huang et al. showed that the use of melt quenching, with $45Li_2O$+$50B_2O_3$+$5Nb_2O_5$ (mol%) and Li_2CO_3 and H_3BO_3 as starting materials, forms transparent and homogeneous glasses without crystalline phases.[57] Prasad[40] also described the application of thermal treatments to lithium borate glasses with niobium, where the $LiNbO_3$ phase was detected for treatments at temperatures above 500°C. In glasses with higher niobium content, the heat-treatment process favors the formation of the Li_3NbO_8 phase, and the value of the dielectric constant appears to increase with increasing volume fraction of $LiNbO_3$. For glasses treated at temperatures above 500°C, the presence of spherical particles, with an average size of 25 nm that increases with increasing thermal treatment temperature, were observed.[40]

Glass-ceramics—Impact of crystalline phases and crystal orientation

Many of these studies have found that the crystalline phases in glass-ceramics fabricated by heat treatment are not orientated along a preferred direction. Typically, if the starting material is an isotropic glass, nucleation and crystal growth will also be isotropic. Because certain physical properties, such as piezoelectricity, depend upon the crystal or domain orientation, the crystal[58] and domain orientations should align along their preferred directions, where alignment for both can be induced though electrical poling.[59,60]

The crystallization process of a particular crystalline phase oriented in a predefined direction is usually difficult to implement because these materials systems require a high electric field value such that the resultant force can overcome the viscous medium, which is characteristic for each glass matrix.

To prepare the crystalline phase oriented in a preferential direction, special techniques must be implemented, such as electrochemically induced nucleation. This consists of applying a constant electric potential difference between two electrodes, which are in contact with the melt, promoting the movement of constituents in the melt in a nonrandom manner. Gerth et al.[58] used this technique in silicate glasses containing lithium and niobium oxides, concluding that $LiNbO_3$ crystallized with a preferred orientation perpendicular to the electrodes. Davis et al.[59] described the preparation of three lithium silicate glass-ceramics—with boron and SiO_2, with $NaNbO_3$, and with $KNbO_3$. The first glass composition is nonferroelectric, but due to its composition, tends to form $Li_2Si_2O_5$ crystals in a preferred direction through a heat-treatment activating process. The second and third examples exhibited ferroelectric characteristics through crystallization of niobate phases. All three glass-ceramics were electrically poled using a potential of approximately 8 kV (1-mm thickness). The piezoelectric properties evaluated in the $Li_2Si_2O_5$ glasses remained undiminished at least up to 600°C, which was the limit of measurement, thus this glass is an example of a piezoelectric material able to function at high temperatures. Reznitchenko et al.[61] mentioned that glass-ceramics with ferroelectric $NaNbO_3$-poled crystals presented a d_{33} coefficient of 15 pC/N, considerably lower than the value of 50 pC/N in dense $NaNbO_3$ ceramics. The d_{33} piezoelectric coefficient, or piezoelectric modulus, quantifies the volume change in the same direction of the applied electric field.

Another technique to control the crystal orientation is to apply an electric field during devitrification of the glass. Zeng et al.[62] showed that the composition $50SiO_2$-$25Li_2O$-$25Nb_2O_5$ (mol%) prepared by melt quenching gives a transparent glass; they observed the crystallization of the $LiNbO_3$ phase with a heat treatment at 800°C for 30 minutes. Upon applying an electric field during the thermal process and cooling the melt to room temperature, dark brown zones appeared in the glass indicating the occurrence of chemical and structural transformations. This suggests the occurrence of an oxidation–reduction reaction activated by the external electric field.

Gerth et al. conducted a similar study in a glass composition $35SiO_2$-$45Li_2O$-$20Nb_2O_5$ (mol%) at 50 mA DC through the melt. Their results suggest that the presence of an external electric field favors nucleation and subsequent crystallization in areas close to the cathode. The $LiNbO_3$ crystallites were isotropically distributed with the *c*-axis perpendicular to the electrode.

Graça et al. presented[41–44,63–69] the structural, morphological, and electrical analyses of silicate, phosphate, and borate base glasses, prepared by melt quenching and sol-gel, where $LiNbO_3$ crystallites were grown by heat treatment with and

https://doi.org/10.1557/mrs.2017.32 Published online by Cambridge University Press

without the presence of an external electric field. **Figure 3**a–b shows micrographs of silicate glasses heat-treated without the presence of an external electric field, revealing $LiNbO_3$ particles with sizes of 60–300 nm embedded in the matrix. Figure 3c shows the micrograph of a silicate glass thermoelectric heat-treated with an external electric field of 5 kV/cm, revealing the growth of crystallites with a preferential orientation.

The preparation of transparent glasses and growth of $LiNbO_3$ crystals in glass networks was thus achieved by heat treatments. Graça et al. showed[41–44,63–69] that the infrared spectra of this type of glass revealed the existence of vibrations associated with NbO_6 octahedral (centered at 595 cm^{-1}) and Si-O- (NBO) bonds (900 cm^{-1}), but they did not provide information on structural modifications of the glass when subjected to heat treatment. However, Raman spectroscopy revealed band narrowing with increasing heat-treatment temperature, indicating devitrification, as also corroborated by XRD data.[41–44,63–69]

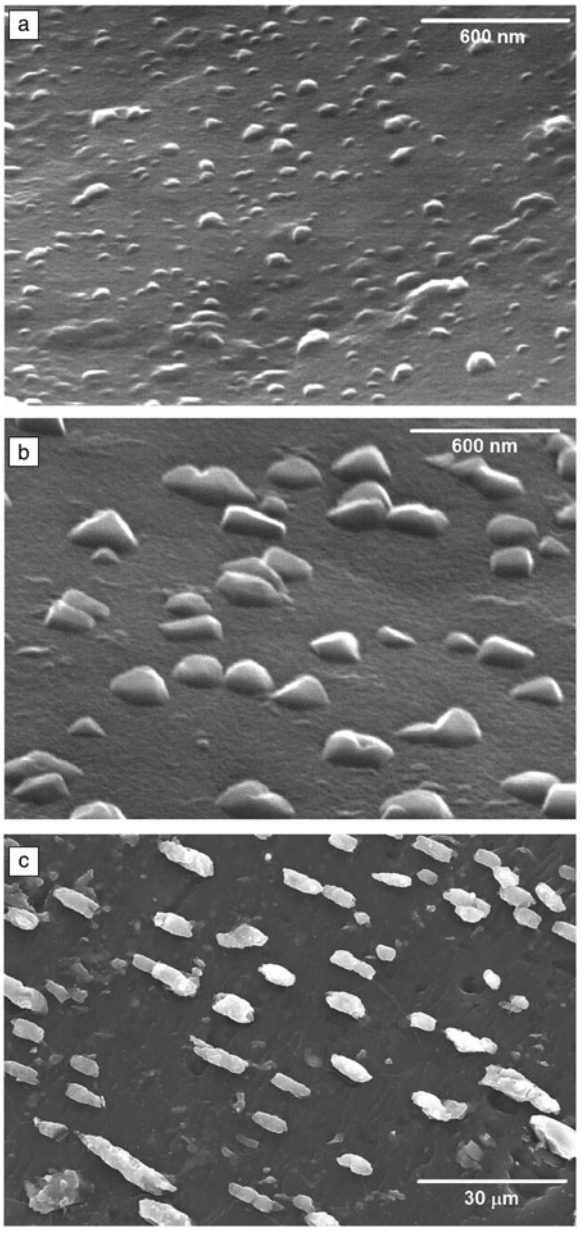


Figure 3. Scanning electron microscope micrographs of samples (a) $34SiO_2$-$33Li_2O$-$33Nb_2O_5$ treated at 500°C; (b) $34SiO_2$-$33Li_2O$-$33Nb_2O_5$ treated at 550°C; and (c) $92SiO_2$-$4Li_2O$-$4Nb_2O_5$ treated at 700°C with a field of 5 kV/cm.[41,63]

From morphological analysis, the modification of the number and size of the particles as a function of the heat-treatment temperature is justified by the diffusion of the network modifier ions (Li^+ and Nb^{5+}), which are structurally inserted in the glass network. Increasing the heat-treatment temperature enables the diffusion of free ions in the glass matrix and causes an increase in the volume of the particles. The electrical analysis assumes the existence of two major contributions, the first associated with the ions structurally inserted in the glass matrix and the second with the particles embedded in the glass matrix.[40] Thus, a decrease in the conductivity is expected, with the increase in crystal volume fraction. The other possible contribution includes the glass matrix and the embedded particles, which can be neglected for the conduction mechanisms due to their high resistivity characteristics. In these glass matrices, the electrical conduction mechanism can be interpreted using the Taylor and Stevels model.[70–72] This model assumes that the ions structurally inserted in a vitreous matrix and responsible for the conductivity are within potential wells (**Figure 4**), and the activation energy represents the energy required by the ion to overcome the potential barriers.

The dielectric measurements of these glasses gives an indication of the quality of the ferroelectric response. In the case of silicate glasses prepared by Graça et al.,[41–44,63–69] a decrease in the dielectric constant (ε′) with an increase in the heat-treatment temperature was observed, which raises two questions. The first is related to the type of dipoles present in these glasses, which can be divided into two groups, one arising from network modifier ions and the other from the particles embedded in the glass matrix. The second question is related to the value of the applied electric field (1 kV/m). These issues suggest that the decrease of ε′ can be attributed to a decrease in the amount of network modifier ions, causing a decrease in the dipole moment. However, given the presence of $LiNbO_3$ ferroelectric crystallites embedded in the glass matrix, it can be assumed that the decrease of ε′ is also influenced by the orientation of the particle dipoles. If the orientation is not completely guided by the applied electrical field, the overall dipole moment will decrease. Knowing that the conventional heat-treatment process promotes crystallite growth in random directions, the possibility of different directions of dipoles is possible, and thus, the dipole moment should decrease.

This hypothesis was confirmed in thermoelectrically treated glasses.[42,66] **Figure 5** illustrates this hypothesis, with the signals (+, –) representing the ions structurally inserted in the glass matrix, decreasing in amount with an increase in

https://doi.org/10.1557/mrs.2017.32 Published online by Cambridge University Press

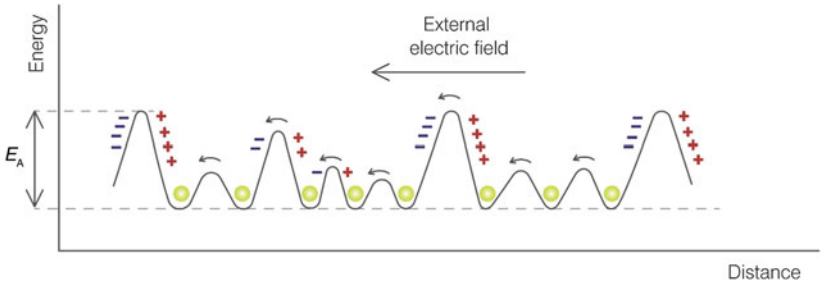


Figure 4. Schematic representation of the model proposed by Stevels and Taylor for the ionic conductivity and polarization. + and – symbolize zones of positive and negative charge accumulation, respectively. The spheres represent charge carriers. Note: E_A, activation energy.[72]

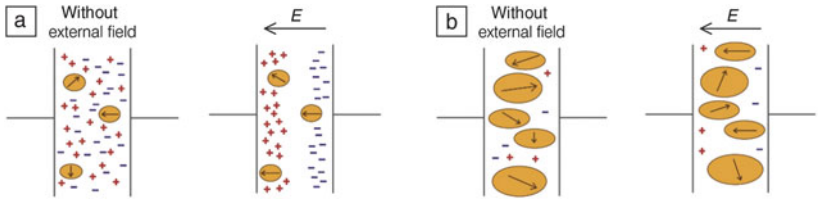


Figure 5. Dielectric model for the glass-ceramics. (a) Glass-ceramic where the free ions are the predominant dielectric units; and (b) glass-ceramic where the embedded crystals are the predominant dielectric units. The signals represent the ions (+, –) structurally inserted in the matrix network, and the arrows represent the dipole orientation from embedded crystals (orange ovals). Note: *E*, electric field.

the heat-treatment temperature and the "circles" representing particles; the dipole orientation is indicated by the arrow.

Summary

This article described the preparation of glass-ceramics with ferroelectric crystals dispersed in a glass matrix. An overview of highlights of various studies conducted thus far are presented, focusing on the type of oxide used as the network former and the methods of formation of the glass-ceramic. The importance of factors such as crystallinity, size, and amount of the particles dispersed in the matrix and the crystallites growth orientation toward the electrical properties were discussed.

Acknowledgments

This work was funded by FEDER funds through the COMPETE 2020 Programme and National Funds through FCT—Portuguese Foundation for Science and Technology under the Project UID/CTM/50025/2013.

References

1. J. Curie, P. Curie, *C. R. Acad. Sci.* **91**, 294 (1880).
2. W.G. Cady, "Report to the National Research Council" US Government Printing Office, (Washington, DC, May 1918).
3. J.A. Anderson, "Report to the National Research Council" US Government Printing Office, (Washington, DC, April/May 1918).
4. J. Valasek, *Phys. Rev.* **17** (4), 475 (1921).
5. G.A. Smolenskii, *Ferroelectrics* **53** (1), 129 (1984).
6. Y. Xu, *Ferroelectric Materials and Their Applications* (Elsevier, Amsterdam, The Netherlands, 1991).
7. F. Jona, G. Shirane, *Ferroelectric Crystals* (Dover, New York, 1993).
8. G.A. Samara, *J. Phys. Condens. Matter* **15** (9), R367 (2003).
9. G.A. Samara, *Solid State Phys.* **56**, 239 (2001).
10. S. Chattopadhyay, *Phys. Rev. B Condens. Matter* **52** (18), 13177 (1995).
11. C. Ziebert, H. Schmitt, J.K. Krüger, A. Sternberg, K.-H. Ehses, *Phys. Rev. B Condens. Matter* **69**, 214106 (2004).
12. R. Blinc, *Ferroelectrics* **267**, 3 (2002).
13. M.M. Aboulleil, F.J. Leonberger, *J. Am. Ceram. Soc.* **72**, 1311 (1989).
14. R.S. Weis, T.K. Gaylord, *Appl. Phys. A* **37**, 191 (1985).
15. G.H. Haertling, *J. Am. Ceram. Soc.* **82** (4), 797 (1999).
16. E. Hecht, *Optics* (Fundação Calouste Gulbenkian, Lisboa, Portugal, 1991).
17. E.M. Vogel, *J. Am. Ceram. Soc.* **72**, 719 (1989).
18. S. Lin, Y. Tanaka, M. Aono, T. Suzuki, *J. Appl. Phys.* **36**, 3510 (1997).
19. J.A.C. Paiva, P.C. Barbosa, J.M. Filho, A.C. Hernandes, J.P. Andreeta, A.S.B. Sombra, *Opt. Mater.* **1**, 59 (1992).
20. P.C. Barbosa, J.A.C. Paiva, J.M. Filho, A.C. Hernandes, J.P. Andreeta, A.S.B. Sombra, *Phys. Status Solidi A* **125**, 723 (1991).
21. J.A.C. Paiva, E.B. Araujo, A.C. Hernandes, A.S.B. Sombra, *Phys. Status Solidi A* **147**, 585 (1995).
22. M. Sorescu, E.T. Knobbe, J.J. Martin, J.D. Barrie, D. Barb, *J. Mater. Sci.* **30**, 5944 (1995).
23. U. Ramabadran, G.N. de Brabander, J.T. Boyd, H.E. Jackson, S. Sriram, "Characterization of Ti:$LiNbO_3$ Optical Channel Waveguides Fabricated Using Rapid Thermal Annealing," *Mater. Res. Soc. Symp. Proc.* **152**, D.B. Poker, C. Ortiz, Eds. (Materials Research Society, Warrendale, PA, 1989), p. 277.
24. T. Nozawa, S. Miyazawa, *J. Appl. Phys.* **35**, 107 (1996).
25. X. Feng, T.B. Tang, *J. Phys. Condens. Matter* **5**, 2423 (1993).
26. I.M. Zaritskii, L.G. Rakitina, *J. Phys. Condens. Matter* **37**, 1073 (1995).
27. M.P.F. Graça, P.R. Prezas, M.M. Costa, M.A. Valente, *J. Solgel Sci. Technol.* **64** (1), 78 (2012).
28. J. Diaz-Caro, J. Garcia-Solé, H. Murrieta, F. Jaque, *J. Lumin.* **72–74**, 177 (1997).
29. R. Burlot, R. Mancongé, G. Bovion, *J. Lumin.* **72–74**, 135 (1997).
30. J.A. Muñoz, R.E. Di Paolo, R. Duchowicz, J.O. Tocho, F. Cussó, *Solid State Commun.* **107** (9), 487 (1998).
31. A. Halliyal, A.S. Bhalla, R.E. Newnham, *Mater. Res. Bull.* **18**, 1007 (1983).
32. Y. Xu, R. Xu, C.-H. Cheng, J.D. Mackenzie, "Electrical Properties of Amorphous Thin Films of Ferroelectric Oxides Prepared by Sol-Gel Technique," *Mater. Res. Soc. Symp. Proc.* **310**, E.R. Myers, B.A. Tuttle, S.B. Desu, P.K. Larsen, Eds. (Materials Research Society, Warrendale, PA, 1993), p. 441.
33. P. Mukherjee, K.B.R. Varma, *Ferroelectrics* **306**, 129 (2004).
34. F. Mehran, B.A. Scott, *Solid State Commun.* **11**, 15 (1972).
35. R. Gerson, J.F. Kirchoff, *J. Appl. Phys.* **60**, 3553 (1986).
36. M.A. Aegerter, *J. Non Cryst. Solids* **151**, 195 (1992).
37. J.M.F. Navarro, *El Vidrio* (Instituto de Ceramica y Vidrio, Madrid, 1985).
38. R. Keding, C. Rüssel, *J. Non Cryst. Solids* **351**, 144 (2005).
39. T. Komatsu, H. Tawarayama, H. Mohri, K. Matusita, *J. Non Cryst. Solids* **135**, 105 (1991).
40. E. Prasad, M. Sayer, H.M. Vyas, *J. Non Cryst. Solids* **40**, 119 (1980).
41. M.P. Graça, M.A. Valente, M.G. Ferreira da Silva, *J. Non Cryst. Solids* **325**, 267 (2003).
42. M.P.F. Graça, M.G.F. Silva, A.S.B. Sombra, M.A. Valente, *J. Non Cryst. Solids* **352**, 5199 (2006).
43. M.P.F. Graça, M.G.F. Silva, A.S.B. Sombra, M.A. Valente, *J. Non Cryst. Solids* **354**, 3408 (2008).
44. M.P.F. Graça, M.A. Valente, M.G.F. Silva, *J. Mater. Sci.* **41**, 1137 (2006).
45. E.B. Araujo, J.A.C. Paiva, M.A.B. Araujo, A.S.B. Sombra, *Phys. Scr.* **53**, 104 (1996).
46. H.G. Kim, T. Komatsu, R. Sato, K. Matusita, *J. Non Cryst. Solids* **162**, 201 (1993).
47. M. Todorovíc, L. Radonjic, *Ceram. Int.* **23**, 55 (1997).
48. T. Komatsu, H.G. Kim, H. Mohri, *J. Mater. Sci. Lett.* **15**, 2026 (1996).
49. M.V. Shankar, K.B.R. Varma, *J. Non Cryst. Solids* **243**,192 (1999).
50. Y. Ding, A. Osaka, Y. Miura, *J. Non Cryst. Solids* **178**, 103 (1994).
51. I. Hasdemir, R. Brückner, J. Deubener, *Phys. Chem. Glasses* **39** (5), 253 (1998).
52. F.L. Galeener, J.C. Mikkelsen Jr., *Solid State Commun.* **30**, 505 (1979).
53. B.V.R. Chowdari, K. Radhakrishnan, *J. Non Cryst. Solids* **110**, 101 (1989).

https://doi.org/10.1557/mrs.2017.32 Published online by Cambridge University Press

54. K. Singh, P.R. Gandhi, B.M. Chaudhari, *Solid State Ionics* **28–30**, 752 (1988).
55. H.L. Tuller, D.P. Button, *Proc. 6th Risø Int. Symp. Metall. Mater. Sci.* (1985), pp. 119–138.
56. A. Paul, *Chemistry of Glasses* (Chapman & Hall, London, 1982).
57. P. Huang, X. Huang, *Solid State Ionics* **36**, 59 (1989).
58. K. Gerth, C. Rüssel, R. Keding, P. Schleevoigt, H. Dunken, *Phys. Chem. Glasses* **40** (3), 135 (1999).
59. M.J. Davis, P. Vullo, I. Mitra, P. Blaum, K.-A. Gudgel, N.J. Donnelly, C.A. Randall, *J. Am. Ceram. Soc.* **91** (9), 2878 (2008).
60. M.J. Davis, *Int. J. Mater. Res.* **99**, 1 (2008).
61. L.A. Reznitchenk, A.V. Turik, E.M. Kuznetsova, V.P. Sakhnenk, *J. Phys. Condens. Matter* **13**, 3875 (2001).
62. H.C. Zeng, K. Tanaka, K. Hiaro, N. Soga, *J. Non Cryst. Solids* **209**, 112 (1999).
63. M.P.F. Graça, M.G.F. Silva, M.A. Valente, *J. Eur. Ceram. Soc.* **28** (6), 1197 (2008).
64. M.P.F. Graça, M.G.F. Silva, A.S.B. Sombra, M.A. Valente, *J. Non Cryst. Solids* **353**, 4390 (2007).
65. M.P.F. Graça, M.G.F. Silva, M.A. Valente, *Solid State Sci.* **11** (2), 570 (2009).
66. M.P.F. Graça, M.G.F. Silva, M.A. Valente, *J. Non Cryst. Solids* **354**, 901 (2008).
67. M.P.F. Graça, M.G.F. Silva, M.A. Valente, *Key Eng. Mater. Adv. Mater. Forum I* **230–232**, 161 (2002).
68. M.P.F. Graça, M.G.F. Silva, M.A. Valente, *J. Mater. Sci.* **42** (8), 2543 (2007).
69. M.P.F. Graça, M.G.F. Silva, A.S.B. Sombra, M.A. Valente, *Physica B* **396** (1–2), 62 (2007).
70. A.K. Agarwal, D.E. Day, *J. Am. Ceram. Soc.* **65** (2), 111 (1981).
71. P.B. Macedo, C.T. Moynihan, R. Bose, *Phys. Chem. Glasses* **13**, 171 (1972).
72. A.K. Jonscher, *Dielectric Relaxation in Solids* (Chelsea Dielectrics Press, London, 1983). □



Manuel Pedro Fernandes Graça is principal researcher at the Institute of Nanostructures, Nanofabrication, and Nanomodeling in the Physics Department and professor of micro- and nanoprocessing techniques at the Universidade de Aveiro, Portugal, since 2008. He obtained his undergraduate degree in physics engineering, master's degree in materials science and engineering, and PhD degree in solid-state physics. His research includes experimental physics and materials electrical properties. He is the author of one book, co-author of seven book chapters, and more than 150 journal articles, with 1400+ citations. Graça can be reached by phone at +351964236731 or by email at mpfg@ua.pt.



Manuel Almeida Valente is the coordinator of the research group Novel Materials and BioSystems at the Institute of Nanostructures, Nanofabrication, and Nanomodeling in the Physics Department at the Universidade de Aveiro, Portugal, where he served as director from 1994 to 1996. He has published one book, five book chapters, 185 articles, and 13 proceedings, with more than 1400 citations. His research interests include magnetic and electric properties, ferroelectric materials, multiferroics, and noncrystalline materials. Valente can be reached by phone at +351234370281 or by email at mav@ua.pt.

INTERNATIONAL CENTRE FOR DIFFRACTION DATA



ICDD databases are the only crystallographic databases in the world with quality marks and quality review processes that are ISO certified.

75 Years Serving the Scientific Community

S Standardized data
M More coverage
A All data sets are evaluated for quality
R Reviewed, edited and corrected prior to publication
T Targeted for material identification and characterization

Featuring
384,613 entries
including
271,449 entries
with atomic coordinates

Visit us at MRS Booth #602

www.icdd.com | marketing@icdd.com

ICDD, the ICDD logo and PDF are registered in the U.S. Patent and Trademark Office.
Powder Diffraction File is a trademark of JCPDS—International Centre for Diffraction Data
©2017 JCPDS—International Centre for Diffraction Data – 2/16

https://doi.org/10.1557/mrs.2017.32 Published online by Cambridge University Press